



Simulation of the Optical Properties of Gold Nanorods : Comparison to Experiment

A.Akouibaa

*Polymer Physics and Critical
Phenomena Laboratory
Sciences Faculty Ben M.sik, P.O.
Box 7955, Casablanca, Morocco*

M.Benhamou

*ENSAM, UniversitéMoulou
Ismail, Meknès, Morocco*

A.Derouiche

*Polymer Physics and Critical
Phenomena Laboratory
Sciences Faculty Ben M.sik, P.O.
Box 7955, Casablanca, Morocco*

Abstract—*The optical absorption spectra of the gold nanorods embedded in a dielectric medium are simulated using finite element method. The study is achieved for various shapes and forms of the nanoparticles and for different values of the dielectric constant of the host medium. Also, we quantify the influence of the aspect ratio and the dielectric constant of the surrounding medium on both longitudinal and transversal resonance modes. It is found that the obtained results are in good agreement with a previous theoretical work that is based on the classical electrostatic predictions and assuming that the gold nanorods behave as ellipsoidal particles. Finally, a comparison of the predicted results with experimental data dealt with the same system is very satisfactory.*

Keyword—*Gold nanorods, Surface Plasmon Resonance, finite element method*

I. INTRODUCTION

The interest in the synthesis of the Gold nanostructures has grown constantly due to their attractive applications in photonics, biological sensing and imaging, and photo-thermal therapy. These interesting applications are mostly based on their unique surface plasmon resonances (SPRs) properties, which originate from the collective oscillation of the electronic conduction at metal surfaces in response to an optical excitation. The resonance frequencies are known to be strongly dependent on the shape, composition, and local environment of particles. Parallel to the experimental efforts, theoretical studies of the optical properties have been carried out for Gold nanostructures with different shapes including nanospheres (e.g. [1], [2]), nanorods (e.g. [3], [4]), nanoshells (e.g. [5], [6]) and nanocages (e.g. [7]). The theoretical predictions are found to be in good agreement with experimentally measured spectra and can be used to interpret the optical effects observed during synthesis.

In addition to the recent interest in the shape control of the nanoparticles, the optical properties of the noble metal particles with their intense colors have fascinated scientists since the turn of this century (e.g. [8], [9]). For example, the spherical Gold nanoparticles show a strong absorption band in the visible region of the electromagnetic field at about 520nm. This absorption, called *plasmon absorption* (e.g. [10], [11]), is absent for very small particles (of diameter 2nm and smaller) as well as for the bulk Gold. It results from the oscillation of the free electrons (6s-electrons of the conduction band in the case of Gold). Mie (e.g. [8]) first described this phenomenon solving theoretically the Maxwell's equations for a radiation field interacting with a spherical metal particle under appropriate boundary conditions (e.g. [8]). Gans (e.g. [9]) extended the Mie's theory to prolate and oblate spheroidal particles averaged over all orientations. For the Gold nanorods, the plasmon resonance then splits into two modes: a longitudinal mode along the long axis of the rod and transversal one perpendicular to the first. The Maxwell-Garnett theory (MGT) or effective medium approach (e.g. [11]-[13]) is also often used to describe the optical properties of the metal nanoparticles. Such a theory computes the effective (complex) dielectric function of the composite material consisting of metal nanoparticles and a surrounding medium (host material). From this dielectric function, the refractive index and the absorption can be calculated. The shape of the particles can be included in this theory through the introduction of a screening parameter. Foss and coworkers (e.g. [14], [15]) have used and modified MGT to model the absorption spectra of the Gold nanoparticles with shapes that vary from oblate to prolate. The Gold nanorods are embedded in a porous aluminum oxide membrane, in which they are well separated and aligned parallel to each other. The optical absorption spectrum shows only one plasmon band, which blue-shifts with increasing aspect ratio in agreement with results from simulations.

As shown by both experiments and calculations, the optical absorption spectra of the Gold nanorods show *two* resonance modes, transversal mode (T-mode) and longitudinal mode (L-mode), corresponding to the electron oscillation associated with the short and long axes of the nanorod, respectively.

In order to simulate the plasmon behavior, several methods have been developed, namely the finite-difference time-domain (e.g. [16]), Fourier pseudo-spectral time-domain (e.g. [17]), multiple multipole (e.g. [18]), volume integral equations with dyadic Green's function (e.g. [19]), boundary-element (e.g. [20]-[22]), surface integral (e.g. [23]), and others. The discrete dipole approximation (DDA) method (e.g. [24]) has been extensively developed in the past few years for the specific study of the spherical nanoparticles. Recently, a number of groups have compared the optical properties

obtained from experiments and DDA simulations for silver nanoprisms (e.g. [25]), silver nanodisks (e.g. [26]), and copper nanocrystals with arbitrary shapes (e.g. [27]). Numerical techniques are designed to solve the relevant field equation in the computational domain, subject to the boundary constraints imposed by the geometry. Without making a priori assumption about which the field interactions are most significant, the numerical techniques analyze the entire geometry provided as input. FEM (e.g. [28]) that is a powerful numerical tool has been widely used for modeling the electromagnetic wave interaction with complex materials. Recently, Benhamou et al. (e.g. [29], [30]) have used this method to study the effects of the polymeric shell on the plasmonic resonance of nanogolds (of arbitrary geometry). The main purpose of this paper is to present various numerical results (in the quasi-static limit) of the absorption cross-section computed using FEM, for a periodic composite structure in which the inclusions are nanorods. The calculated data are compared with experimental results. The effect of the aspect ratio (height/diameter) is then observed. The influence of the dielectric constant of the surrounding medium is also studied.

The remaining presentation proceeds as follows. Sections 2 and 3 summarize previous works dealing with the calculation of the absorption spectrum and the effective permittivity of the Gold nanoparticles with different shapes (sphere, ellipsoid), and the technique used to compute the relevant parameters of the problem. Formulae for calculating the optical properties like effective permittivity and absorption cross-section for Au nanorods, are recalled in Section 4. We describe, in Section 5, the used numerical methodology and computational aspects. Discussion of results is the aim of Section 6. Finally, some concluding remarks are drawn in the last section.

II. OPTICAL PROPERTIES OF GOLD NANORODS

The purpose is to describe the optical properties of the metal nanoparticles, in particular, the Gold nanorods. We focus on the optical properties relevant to multiplexed optical recording, namely the wavelength and polarization sensitivity of SPRs. Prior to the explanation, a short glance back will be given and the theoretical models of Mie, Gans and Drude model (DM) (e.g. [31]) with *Two Critical Point* (TCP) will be shortly described, because of their importance to the field of plasmonics.

II.1. Mie's theory

The problem of the absorption and scattering of light by spherical particles of arbitrary size was first treated by Mie, in 1908 (e.g. [8]). The author described theoretically the mechanism for the absorption of light by small metal particles solving the Maxwell's equations. The theory is based on an assumption that the interactions of the electromagnetic field with the particle induce a charge separation on its surface. This charge separation is a cause for an occurring restoring force. It has been shown that such absorption of light in the UV-Visible region by the metal particles is sensitive to many geometrical, as well as environmental factors (e.g. [32]). Solving Maxwell's equations leads to a relationship for the extinction cross-section for metal nanoparticles, that is

$$\sigma_{ext} = \sigma_{abs} + \sigma_{sca} , \quad (1)$$

where the quantities σ_{ext} , σ_{abs} and σ_{sca} denote the extinction, absorption and scattering cross-section, respectively.

If the particle radius, R , is small in comparison to the light wavelength, λ , then, only the absorption is significant. For the description of the optical properties of nanorods, we shall need the complex expression of the dielectric constant,

$$\varepsilon(\omega) = \varepsilon'(\omega) + \varepsilon''(\omega) . \quad (2)$$

Here, $\varepsilon'(\omega)$ and $\varepsilon''(\omega)$ are the real and imaginary part of the dielectric function of the metal nanoparticles, respectively, and ω is the angular frequency of the exciting radiation according to DM (e.g. [31]). Based on the assumptions that the particles are spherical, small and embedded in an isotropic and non-absorbing medium with a dielectric constant given by $\varepsilon_m = n_m^2$ (n_m being the corresponding refraction index), Mie calculated the extinction cross-section and found that its real part is

$$\sigma_{ext}(\omega) = 9 (\omega/c) \varepsilon_m^{3/2} V_0 \frac{\varepsilon''(\omega)}{[\varepsilon'(\omega) + 2\varepsilon_m]^2 + \varepsilon''(\omega)^2} , \quad (3)$$

where $V_0 = (4\pi/3)R^3$ is the volume of the spherical nanoparticle, c is the vacuum velocity of light, and ε_m accounts for the dielectric constant of the host medium.

The above equation determines the shape of the absorption band of particles. The band width and the peak height are well approximated by $\varepsilon''(\omega)$. The position of the maximum absorption occurs when $\varepsilon'(\omega) \approx -2\varepsilon_m$, if $\varepsilon''(\omega)$ is small or if it is only weakly dependent on ω . One can also see from Eq. (3) that no size-dependence of the peak position is predicted. Contrary to the theory, the size-dependence is observed in many experimental results (e.g. [33]-[35]). From this equation, one can deduce two limiting cases for which σ_{ext} is equal to zero. In the first case, the complex part of the dielectric constant is zero ($\varepsilon''(\omega) = 0$), that is the particle is non-absorbing. This is the case of dielectric materials, as quartz or sapphire, which do not absorb in the visible-range. It is why they are used as substrates for the transmission measurements. In the second case ($\varepsilon''(\omega) \rightarrow \infty$), however, the material reflects all of incoming radiation at this wavelength, that is the complex part of the dielectric function for metals has a large value in the visible making them very shiny and totally reflecting for the incoming light. Since the shape of the nanoparticles is not limited to spherical, the Mie's model had to be extended to other morphologies.

II.2. Gans's theory

In 1912, Gans (e.g. [9]) presented his modification of the Mie's theory, which extended the expression of the extinction cross-section of spheres to ellipsoidal particles. Due to the ellipsoidal shape, the surface plasmon mode would split into two distinct modes. The first is along the short axis of the ellipsoid, while the second is rather along the long axis. The authors quantified the response as a function of the ellipsoid aspect ratio. *Electron Microscopy* revealed that most nanorods are more like cylinders or sphero-capped cylinders than ellipsoids. However, an analytical solution for such shapes is not possible. Solutions have been found for the case of an infinite cylinder and for oblate and prolate ellipsoids. Ruppin has published a number of studies dealt with scattering light from finite dielectric cylinders (e.g. [36], [37]). In the same context, Fuchs has determined numerically the modes of cube-shaped nanocrystals (e.g. [38]) and non-spherical particles, using the surface integral technique that appears to be an alternative to DDA approach. Numerical methods, especially the T-matrix (e.g. [39], [40]) and DDA techniques (e.g. [41]-[43]) have been applied to small particles. Schatz and coworkers (e.g. [24]) have recently reviewed this approach.

The extinction cross-section proposed by Gans, considered an ellipsoid whose dimensions fulfill the condition that $a > b = c$, as shown in Fig. 1. Its expression is as follows

$$\sigma_{\text{ext}} = \frac{\omega}{3c} \epsilon_m^{3/2} V_e \sum_j \frac{(1/L_j^2) \epsilon''(\omega)}{\left[\epsilon'(\omega) + \frac{1-L_j}{L_j} \epsilon_m \right]^2 + \epsilon''(\omega)^2}, \quad (j = x, y, z), \quad (4)$$

where L_j 's are the depolarization factors along the three axes of the ellipsoid, and $V_e = (4/3)abc$ is its volume. In this case, $b = c$, thus $V_e = (4/3)ab^2$.

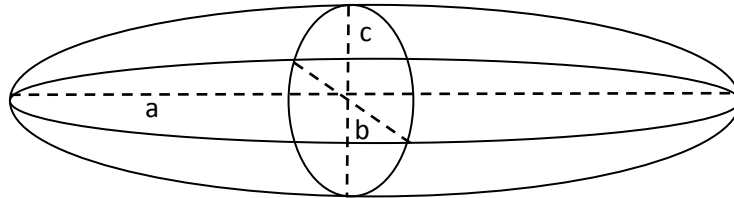


Fig. 1: Schematic of an ellipsoidal particle with dimensions (a, b, c) , such as $a > b = c$, where a is the dimension of the longitudinal axis, and b and c are the dimensions of the transverse axes.

The depolarization factors L_j 's express the force that seeks to restore the initial electron distribution along each of the ellipsoid axes (e.g. [44]). They are defined as follows (e.g. [45])

$$L_x = \frac{1-e^2}{e^2} \left[\frac{1}{2e} \ln \left(\frac{1+e}{1-e} \right) - 1 \right], \quad (5)$$

$$L_y = L_z = \frac{1-L_x}{2}. \quad (6)$$

Here, e is the ellipticity of ellipsoid, which refers to its aspect ratio (*long axis/short axis*). It is defined by

$$e = \sqrt{1 - (b/a)^2}. \quad (7)$$

The theory developed by Gans predicts that SPR would split into two modes (longitudinal and transversal), due to the independent polarizability along the respective particle axes. Because of the difficulty in preparing nonspherical particles, little experimental works to support Gans formulation existed until 1950. In 1960, Stookey *et al.* (e.g. [46]) stretched glasses containing small silver spheres and found that the small particles were elongated in the glass and exhibited red-shifted absorption spectra. More recently, it has become possible to prepare large amounts of small Gold rods in aqueous solution (e.g. [47]-[51]). By varying the chemical composition in the solution, the aspect ratio can be tuned from 2 to as much as 50. In the vast majority of these studies Gans' theory has successfully explained the qualitative optical properties of the Gold nanorods.

III. EFFECTIVE MEDIUM THEORY

III.1. Effective dielectric constant

Several theories have been developed to describe the optical properties of the metal inclusions in a dielectric matrix, among the most important; there is MGT (e.g. [13]). Such a theory allows the computation of the effective dielectric function of a medium, with very low-volume fraction dispersed metal spheres (the mutual interactions between these particles are practically absent).

In some cases, the volume concentration of the nanoparticles is too high, so that the so-called effective medium approximation is reliable. This approximation serving as a model for the computation of the dielectric constant of a nanocomposite, in quasi-static limit, assumes that the incorporated particles are very small compared to the light wavelength, that is $R \ll \lambda$. In this limit, the scattered light is negligible with respect to as absorption by the particle. Effective dielectric permittivity, ϵ_{eff} , must satisfy the equation of the electric displacement (e.g. [52]), that is

$$\vec{D} = \epsilon_{eff} \vec{E}_{int} = \epsilon_m \vec{E}_{int} + \vec{P}, \quad (8)$$

where \vec{P} is the macroscopic polarization vector that can be connected to the polarizability of the inclusions, α , by

$$\vec{P} = N\alpha\epsilon_m \vec{E}_l. \quad (9)$$

Here, ϵ_m accounts for the dielectric permittivity of the medium with immersed inclusions, of number density N . There, \vec{E}_{int} and \vec{E}_l are the internal and local fields, respectively. These quantities are related by

$$\vec{E}_l = \vec{E}_{int} + N\alpha\vec{L}\vec{E}_l. \quad (10)$$

The second contribution in the *r.h.s* of this equality denotes the depolarization term, where \vec{L} is the depolarization tensor that naturally depends on the geometric shape of inclusions.

Combining Eqs. (8), (9) and (10) leads to the expression of the effective dielectric permittivity. In the case of an anisotropic medium where the nanoparticles present a dissymmetry and are randomly oriented in space, the effective permittivity is given by

$$\epsilon_{eff} = \epsilon_m \left(1 + \frac{N\alpha_i}{1 - N\alpha_i L_i} \right), \quad i = (x, y, z), \quad (11)$$

where α_i and L_i are the polarizability and depolarization factor of the nanoparticle in space-direction j . In the case of a spherical nanoparticle, the polarizabilities are equal along the three axes, that is ($\alpha_x = \alpha_y = \alpha_z = \alpha$) and $L_x = L_y = L_z = 1/3$.

In the case where the particle has a spheroid shape, the depolarization factor in space-direction j are defined in Eqs. (5) and (6), while the associated polarizability reads

$$\alpha_i = 4\pi abc \frac{(\epsilon - \epsilon_m)}{3\epsilon_m + 3L_i(\epsilon - \epsilon_m)}, \quad i = (x, y, z). \quad (12)$$

Therefore, to calculate the effective permittivity, using Eqs. (11) and (12), one must know the expression of the polarizability of each inclusion solving the Laplace's equation, in the quasi-static limit. Analytical expressions were obtained for simple geometric shapes (sphere and ellipsoid), in the case of low-density inclusions (dispersed phase).

In this work, we aim at the study of the optical properties of Gold nanorods immersed in a dielectric medium. To this end, we first regard these nanorods as cylinders. However, an analytical solution for these shapes is not possible. Then, this requires would a numerical solution using FEM.

III.2. Dielectric function of nanogolds

The optical response of a metal is quantified by its dielectric constant. The latter is a function of frequency of the electromagnetic wave with which it interacts. Indeed, the interaction of an electromagnetic wave with a pulse, ω , with a metal will lead to a polarization of the medium. This polarization will then generate a change in the complex refractive index, $\tilde{n}(\omega)$, which is related to the dielectric constant by

$$\tilde{n}^2(\omega) = \epsilon(\omega). \quad (13)$$

In the case of metal nanoparticles, the electronic properties appear when their size is smaller than the mean free path of electrons. From a classical point of view, this corresponds to the fact that the electron-surface collisions are not negligible compared to other interaction processes (electron-electron, electron-phonon) and must be taken into account in the rate of the optical collision of electrons.

To well model the interaction of an electromagnetic wave with a Gold nanoparticle, several models are developed to express the dependence of the dielectric constant on wave frequency. Among these, we can quote phenomenological DM (e.g. [31], [34], [53]-[56]) and Drude-Lorentz model (DLM) (e.g. [57]). Each has its advantages and weaknesses. The first ignores the interband transitions, while these transitions are possible when the incident photon energy exceeds a certain threshold. DLM best describes the dielectric function of Gold, only in the frequency band between 0.5eV and 3.5eV. In order to describe the permittivity of Gold in a wide frequency band, use was made of DM with TCP (e.g. [58]). This model is valid in the frequency band between 0.5eV to 6.5eV corresponding to wavelengths between 200nm and 2400nm. Within the framework of this model, the permittivity of a Gold nanoparticle is expressed by

$$\epsilon = \epsilon_\infty - \frac{\omega_D^2}{\omega^2 + i\gamma\omega} + \sum_{j=1}^2 A_j \Omega_j \left(\frac{e^{i\Phi_j}}{\Omega_j - \omega - i\Gamma_j} + \frac{e^{-i\Phi_j}}{\Omega_j + \omega + i\Gamma_j} \right). \quad (14)$$

In this relationship, ϵ_∞ is the permittivity at infinite frequency, ω_D is the frequency of the volume plasmon, γ is the collision rate of electrons, and the third contribution in the *r.h.s* of the above relation represents the Lorentz term.

IV. ABSORPTION COEFFICIENT AND EFFECTIVE DIELECTRIC FUNCTION

From the evolution of the effective complex dielectric function depending on the wavelength or frequency of the incident field, the resonance modes that may occur in the nanorods, are identified.

Let n_{eff} and κ_{eff} the refractive and extinction indices of the composite material that is a dielectric medium with immersed Gold nanorods. We easily obtain the relationship between these two indices and the imaginary part of the dielectric function,

$$\kappa_{eff} = \frac{1}{2n_{eff}} \text{Im}(\epsilon_{eff}). \quad (15)$$

In the case where the particle dimensions are very small compared to the wavelength, the light scattering is negligible. Therefore, the attenuation factor of the composite is called absorption coefficient whose expression is

$$C_{abs} = \frac{2\omega}{c} \kappa_{eff}. \quad (16)$$

It should be noted that the absorption coefficient is a quantity characterizing the optical properties of material. This factor can be determined from the imaginary part of the effective permittivity. The evolution of the imaginary part of the effective permittivity upon frequency of the incident wave represents the optical extinction spectrum.

In the limit where the inclusions of dimensions less than the wavelength, each metal inclusion is supposed to act independently, and contributes linearly with the total extinction of the nanocomposite. The absorption coefficient, through the number density, N_{inc} , of the absorbent inclusions, writes

$$C_{abs} = N_{inc} \sigma_{abs}. \quad (17)$$

The absorption cross-section, σ_{abs} , can be determined from the imaginary part of the effective dielectric function of the composite, through the relationship (e.g. [58]),

$$\sigma_{abs} = \frac{V_p}{f} \frac{k}{n_{eff}} \epsilon_{eff}'' \quad (18)$$

Here, V_p stands for the common volume of nanoparticles, f is their fraction, k is the wave-vector amplitude of the electromagnetic wave, and n_{eff} represents the refractive index that can be related to the real and imaginary parts, ϵ_{eff}' and ϵ_{eff}'' , of the effective permittivity by (e.g. [59])

$$n_{eff} = \left(\frac{\sqrt{\epsilon_{eff}'^2 + \epsilon_{eff}''^2} + \epsilon_{eff}'}{2} \right)^{1/2}. \quad (19)$$

Therefore, the position of the optical resonance peak of these nanostructures is predicted from the effective medium theory, through the imaginary part of the effective permittivity, which can be calculated from FEM. This will be the aim of the next section.

V. NUMERICAL COMPUTATION OF THE EFFECTIVE PERMITTIVITY

Given the progress achieved in the power of computer processing, understanding the dielectric behavior of the heterogeneous structures has stimulated many theoretical studies that are based on numerical calculations, especially in the case where the inclusions are randomly dispersed in the matrix (e.g. [60]-[63]). For this particular case, the laws governing the dielectric behavior of the composite materials are deduced (e.g. [60]). In order to study some details of the dielectric properties of the periodic composites, in the quasi-static limit, FEM is used for the determination of the effective permittivity. A detailed description of the method can be found in literature (e.g. [62]). We consider a parallel plate capacitor, as shown in Figs. 3a and 3b, which is formed by two metal plates of area $S_d = L_1 \times L_2$ and separated by the height L_3 . The two plates are submitted to a potential difference $V_2 - V_1$.

Solving the problem at hand means finding the local potential distribution inside the unit cell volume solving the first principle of electrostatics, namely the Laplace's equation

$$\vec{\nabla} \left(\epsilon_0 \epsilon(\vec{r}) \vec{\nabla} V(\vec{r}) \right) = 0, \quad (20)$$

where $\vec{\nabla}$ is the first derivative with respect to the position-vector, r , of the representative point of the medium, and $\epsilon(\vec{r})$ and V are the local relative permittivity and the potential distribution inside the spatial domain (with zero charge density), respectively. There, $\epsilon_0 = 8.85 \times 10^{-12} \text{Fm}^{-1}$ is the permittivity of vacuum. The electrostatic energy, W_e^k , and losses, P_e^k , can be expressed in terms of the potential derivatives for each tetrahedral element by

$$W_e^k = \frac{\epsilon_0}{2} \iiint_{V_k} \epsilon_k'(x, y, z) \left[\left(\frac{\partial V}{\partial x} \right)^2 + \left(\frac{\partial V}{\partial y} \right)^2 + \left(\frac{\partial V}{\partial z} \right)^2 \right] dV_k, \quad (21)$$

$$P_e^k = \frac{\epsilon_0}{2} \iiint_{V_k} \omega \epsilon_k''(x, y, z) \left[\left(\frac{\partial V}{\partial x} \right)^2 + \left(\frac{\partial V}{\partial y} \right)^2 + \left(\frac{\partial V}{\partial z} \right)^2 \right] dV_k. \quad (22)$$

Here, ϵ_k and V_k represent the permittivity and the volume of the k th tetrahedron element, respectively. The phases of the composite are described through their complex permittivity $\epsilon_k = \epsilon_k' + i\epsilon_k''$. Periodic boundary conditions $\partial V/\partial n = 0$ are enforced on faces perpendicular to x and y space-directions. Consequently, the edge fringing effects can be eliminated, and then, the effective permittivity of the composite can be determined from energy W_e^k and losses P_e^k stored in the capacitor according to

$$W_e^k = \frac{1}{2} \epsilon_{eff}' \frac{S_d}{L_3} (V_2 - V_1)^2, \quad (23)$$

$$P_e^k = \frac{1}{2} \omega \epsilon_{eff}'' \frac{S_d}{L_3} (V_2 - V_1)^2. \quad (24)$$

Having established the mathematical equation (20) that describes physics, we must point-out how to solve it for the interested domain, with appropriate boundary conditions. In the framework of FEM, the domain is decomposed into a number of uniform or non-uniform finite elements that are connected via nodes. For each subspace element, the function modeling the potential V is defined by a polynomial interpolation function. Then, the boundary values are replaced by an equivalent integral formulation. The interpolation polynomials are then replaced into the integral equation and integrated in the domain of interest. Finally, the results of this step are converted into matrix equation, which is afterward solved for V (e.g. [63], [64]).

FEM is applicable to 2D and 3D composites periodic or not, with or without losses. However, for a random distribution of inclusions, this method is not applicable, because it does not solve a problem with an unclear or a complicated geometry, due to the number of distributed randomly elementary cells. Generally, the plasmonic metal nanostructures inserted in a matrix without loss, used in the field of nanoelectronics or nanooptics, are often periodic.

VI. RESULTS AND DISCUSSION

In this work, we are interested in the study of the optical properties of nanorods from FEM. The geometric anisotropy of these inclusions allows the appearance of two resonance modes. One is longitudinal (L) and the other is transversal (T), which appear depending on the polarization direction of the external field. In figures 2a and 2b, as an illustration, we model a composite 3D by a cell of length L_1 , height L_2 and width L_3 , containing an inclusion. Actually, the inclusions are dispersed in a dielectric medium with arbitrary orientations that lead to the appearance of two resonances L and T-modes, in the same absorption spectrum. In Fig. 2c, we represent the modeling of a composite, with a cell containing three nanorods, one is parallel to the direction of the applied external field (L-mode), the two other are perpendicular to the direction of this field (T-mode).

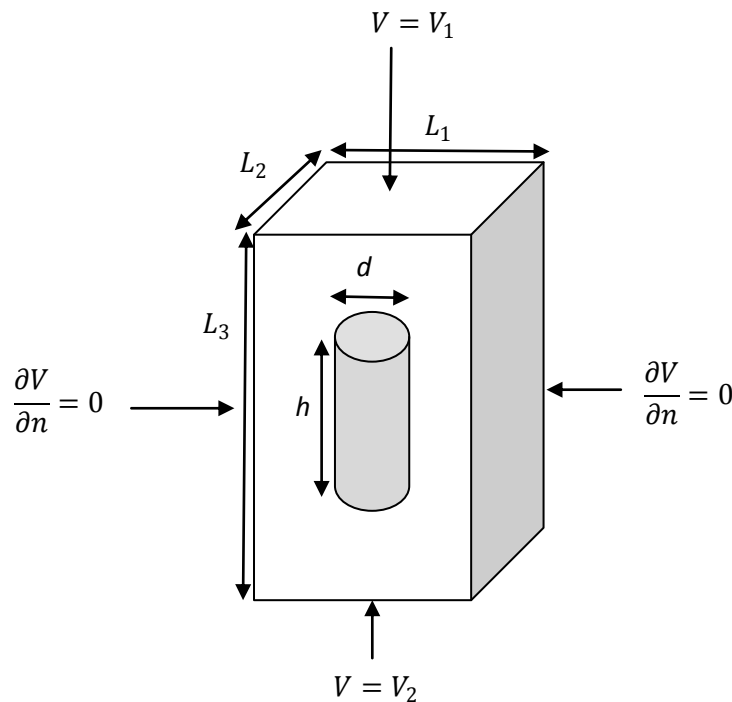


Fig. 2a: Schematic representation of a three-dimensional composite medium by a cell with length L_1 , width L_2 and height L_3 . This cell contains a single nanorod oriented parallel to the applied field. On the boundary of each cell, the potential

V is V_1 on the top face, and V_2 on the bottom one, and its normal derivative, $\partial V/\partial n$, is equal to zero along the vertical walls.

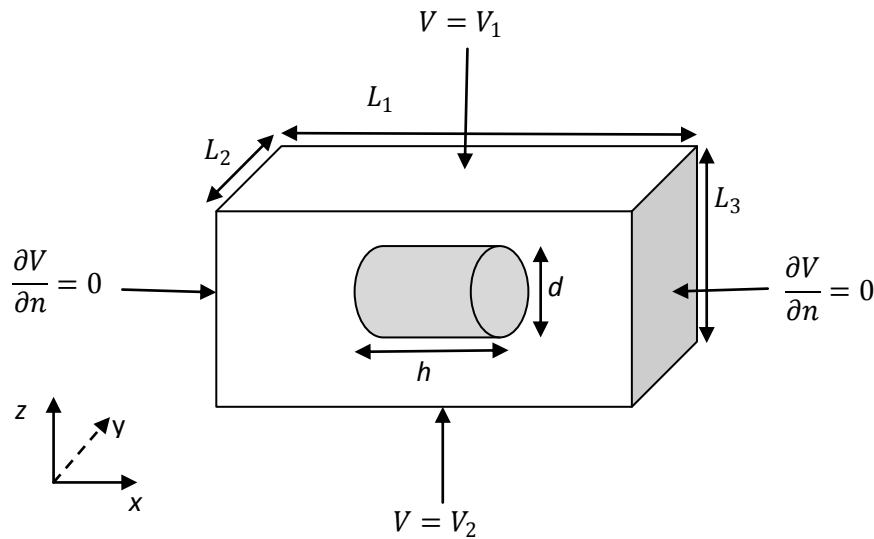


Fig. 2b: Schematic representation of a three-dimensional composite medium by a cell with length L_1 , width L_2 and height L_3 . This cell contains a single nanorod oriented perpendicularly to the applied field. On the boundary of each cell, the potential V is V_1 on the top face, and V_2 on the bottom one, and its normal derivative, $\partial V/\partial n$, is equal to zero along the vertical walls.

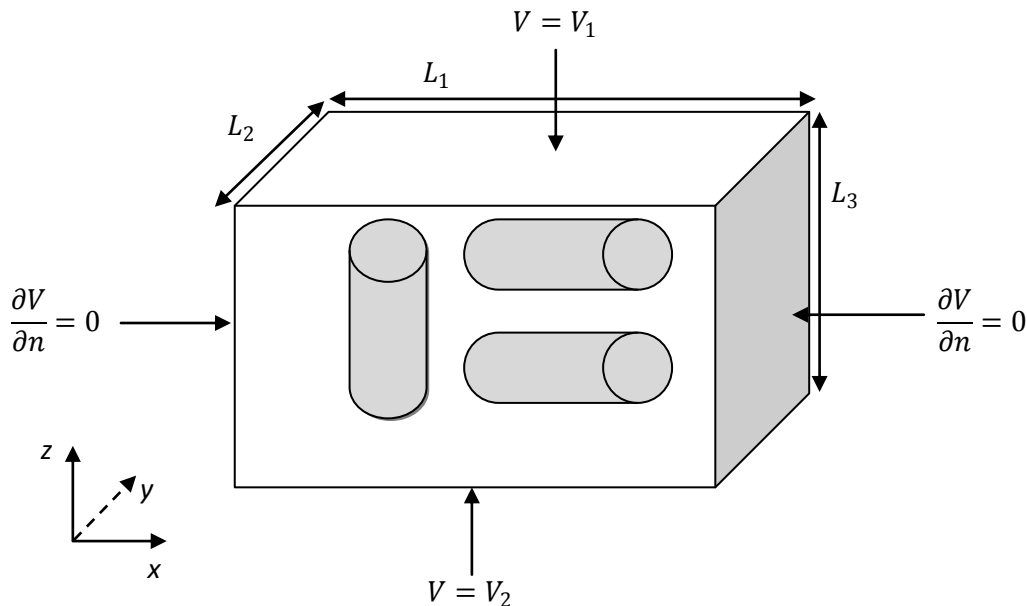


Fig. 2c: Schematic representation of a three-dimensional composite medium by a cell with length L_1 , width L_2 and height L_3 . This cell contains three nanorods one oriented parallelly to the applied field and the two others are perpendicular. On the boundary of each cell, the potential V is V_1 on the top face, and V_2 on the bottom one, and its normal derivative, $\partial V/\partial n$, is equal to zero along the vertical walls.

We consider an isolated nanorod of height $h = 33,5nm$ and diameter $D = 10,2nm$. The aspect ratio of this nanoparticle is $\eta = 3.28$, defined by the ratio of height to diameter, with a volume fraction $\phi_v = 0.125$. The chosen permittivity of the host matrix is $\epsilon_m = 1.77$. We assume that the field is applied either along the height (L-mode excited), or perpendicular to this height (T-mode excited). In Figs. 3a and 3b, we report the variation of the absorption cross-sections upon energy of the incident electromagnetic wave obtained using FEM, for both L and T-modes. These curves show that the two resonance modes appear in the infrared ($E = 1.56eV, \lambda_{max} = 795.85nm$) and blue ($E = 2.40eV, \lambda_{max} = 517nm$) domains. We note that the amplitude of L-mode is much larger than that of T-mode. The

spectrum resonance for arbitrary orientations (polydisperse case) is given in Fig. 3c, in which appear the two spectra. It should be noted that the orientation of such inclusion having certain anisotropy, relative to the applied field, is a factor that strongly influences the resonance spectra.

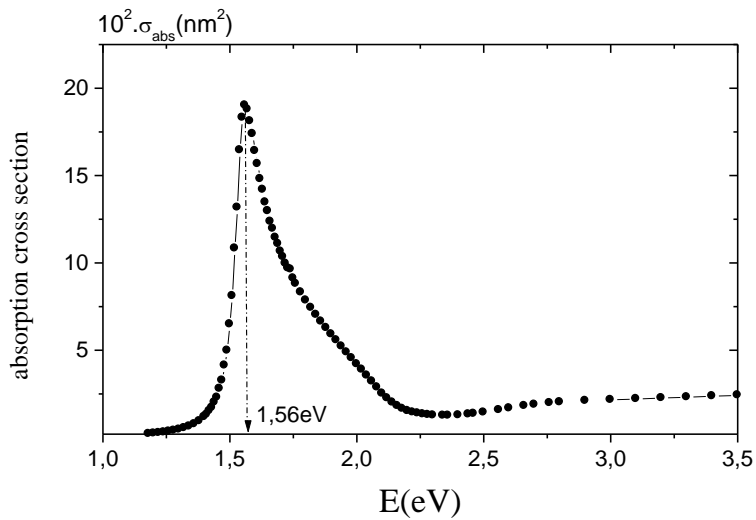


Fig. 3a: Absorption spectrum of L-mode of a Gold nanorod of height $h = 33.5nm$, diameter $D = 10.2nm$, and volume fraction $\Phi_v = 0.125$. The dielectric constant of the medium is fixed to the value $\epsilon_m = 1.77$.

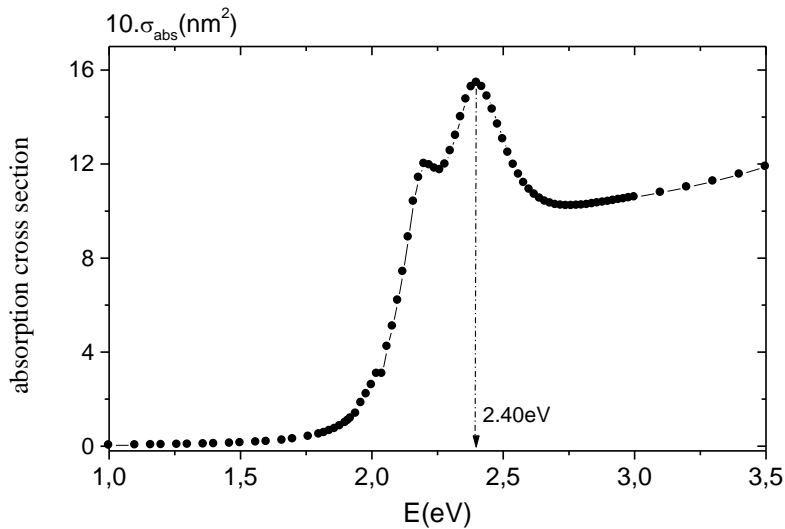


Fig. 3b: Absorption spectrum of T-mode of a Gold nanorod of height $h = 33.5nm$, diameter $D = 10.2nm$, and volume fraction $\Phi_v = 0.125$. The curve is drawn choosing the following value of the dielectric constant of the medium $\epsilon_m = 1.77$.

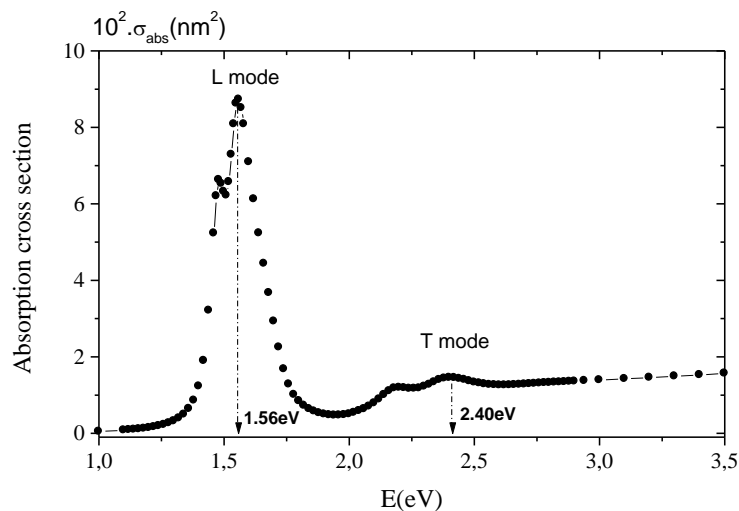


Fig. 3c: Absorption spectrum of mixed orientations nanorods (L-mode and T-mode), with height $h = 33.5nm$, diameter $D = 10.2nm$, and volume fraction $\Phi_v = 0.125$. The dielectric constant of the medium is fixed to the value $\epsilon_m = 1.77$.

In our study, the purpose is the determination of the absorption spectrum of L-mode. For this, we assume that the nanorods are arranged parallelly to the direction of the external applied field. In the following, numerical calculations of the absorption cross-section using FEM method are compared to very recent experiments (e.g. [47], [65], [66]). The major change in the absorption spectrum of Gold nanorods is the position of the well-known L-mode. To see the influence on the maximum resonance, λ_{max} , of the geometrical parameters of nanorods, such as height h , diameter D , and aspect ratio η , a batch of simulations, considering each parameter, is performed. Now, consider a set of nanorods with different geometric parameters (height, diameter and aspect ratio). For the study, the chosen parameters are those of a recent experiment (e.g. [65]), which was concerned with the synthesis of nanorods in aqueous environments (with narrow size distribution) using a seed-mediated method. In this experiment, the size of the nanorods is determined by *Transmission Electron Microscopy*. The optical properties of an assembly of Gold nanorods are studied experimentally through the determination of the absorption spectrum. Table I summarizes the geometrical parameters of nanorods synthesized well as Plasmon Band Position, λ_{max} , of L-mode, experimentally determined. To model the optical properties of these nanorods, via the absorption spectrum of L-mode by FEM method, we consider that each nanorod is placed parallelly to the direction of external field in aqueous environments of permittivity $\epsilon_m = 1.77$. The absorption spectra of a collection of nanoparticles are given in Figs. 4a-4e. These spectra clearly show that, at low energy, the well-known plasmon resonance peak is attributed to the L-mode. This curve shows that the L-mode increase is due to the change in the nanorod lengths from one sample to another.

To compare the results of our simulation method with experimental ones (e.g. [65]), we presented, in Table I, FEM results beside those obtained experimentally. This table reveals that the used numerical method is in good agreement with experiment.

TABLE I
THE REPRODUCED EXPERIMENTAL AND NUMERICAL RESULTS CORRESPONDING TO FIGS 4a-4e

Figures	Length (nm)	Width (nm)	Aspect ratio	Exp. λ_{max} (nm)	Num. λ_{max} (nm)
4a	30.5	9.7	3.14	770	770.18
4b	33.5	10.2	3.28	795	795.85
4c	34.2	10.3	3.32	790	790.28
4d	29	10.7	3.33	792	792.29
4e	35.2	10.1	3.48	798	798.41

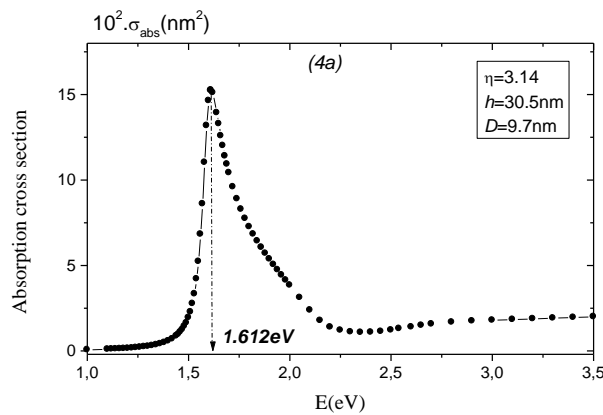


Fig. 4a: Absorption spectrum of L-mode of Gold nanorods with values of heights and diameters ($h = 30.5 \text{ nm}$, $D = 9.7 \text{ nm}$). The curves are drawn choosing : $\epsilon_m=1.77$.

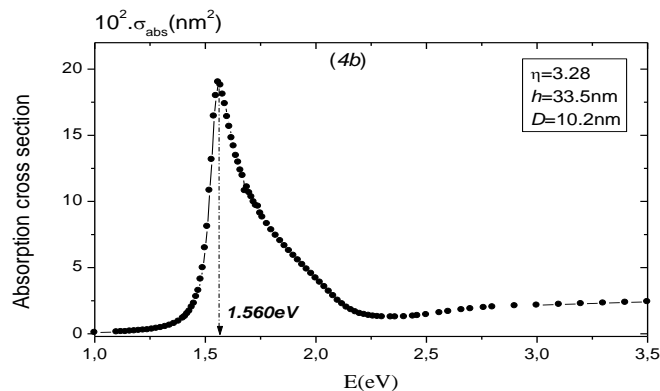


Fig. 4b: Absorption spectrum of L-mode of Gold nanorods with values of heights and diameters ($h = 33.5 \text{ nm}$, $D = 10.2 \text{ nm}$). The curves are drawn choosing : $\epsilon_m=1.77$.

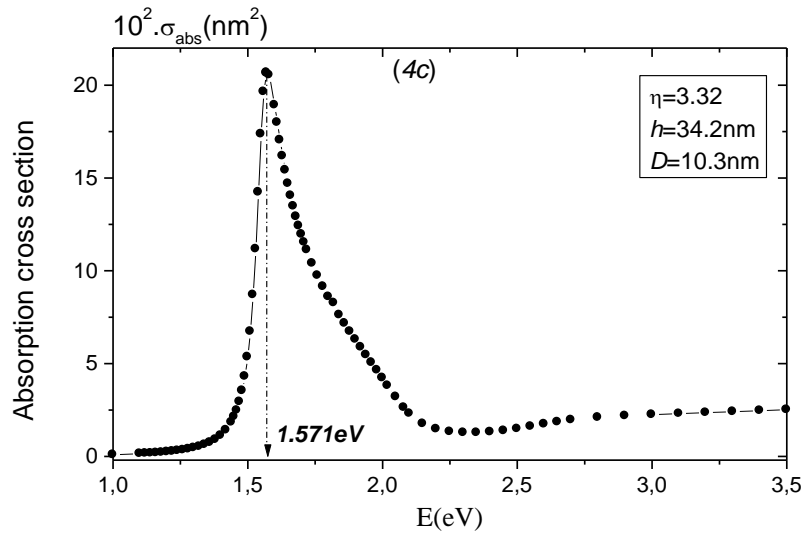


Fig. 4c: Absorption spectrum of L-mode of Gold nanorods with values of heights and diameters ($h = 34.2 \text{ nm}$, $D = 10.3 \text{ nm}$). The curves are drawn choosing : $\epsilon m=1.77$.

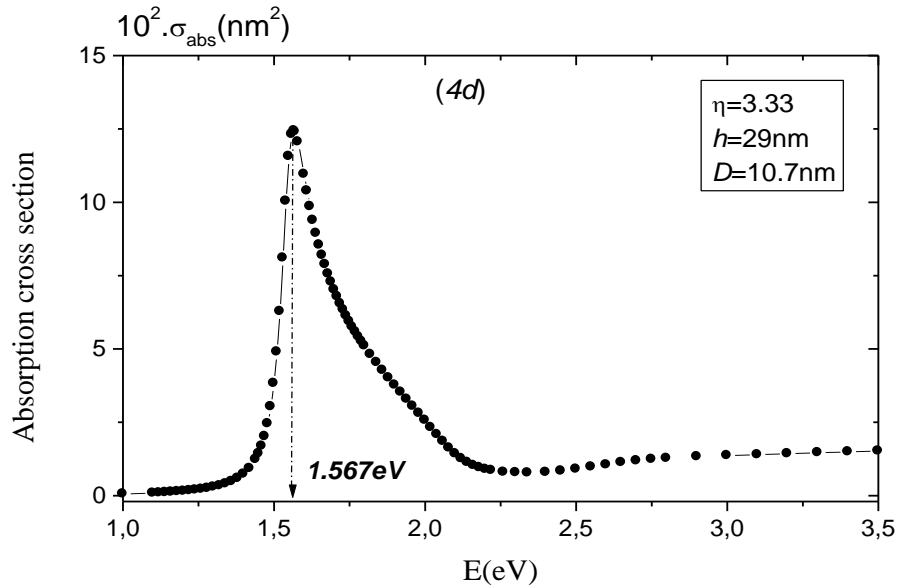


Fig. 4d: Absorption spectrum of L-mode of Gold nanorods with values of heights and diameters ($h = 29 \text{ nm}$, $D = 10.7 \text{ nm}$). The curves are drawn choosing : $\epsilon m=1.77$.

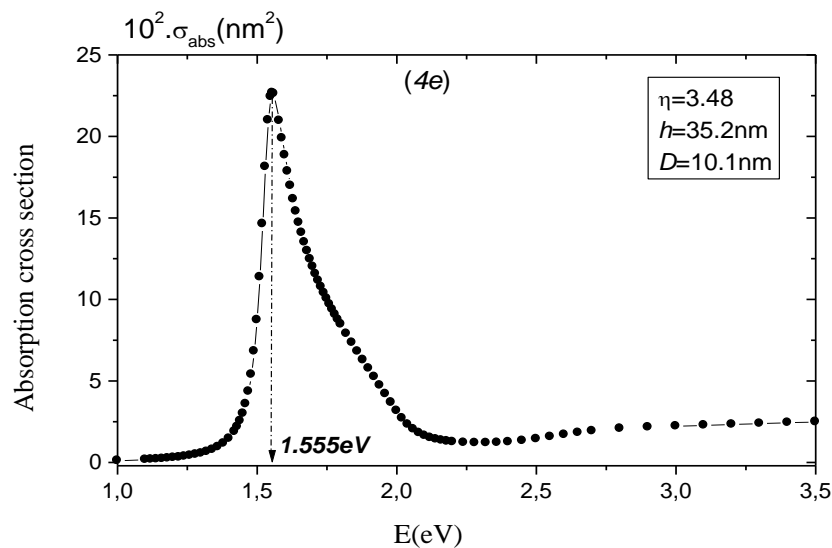


Fig. 4e: Absorption spectrum of L-mode of Gold nanorods with values of heights and diameters ($h = 35.2 \text{ nm}$, $D = 10.1 \text{ nm}$). The curves are drawn choosing : $\epsilon m=1.77$.

The Gans' equation predicts how the plasmon mode peak position varies with the aspect ratio, for small ellipsoids embedded in the same medium. The easiest way to see that is to plot the depolarization factor L , defined in Eq. (5), versus the value of the dielectric function at the peak. To investigate the effects of the aspect ratio on the absorption spectrum of the nanorods using FEM, we consider Gold nanorods having various aspect ratios: $\eta = 2.23$ to $\eta = 5.35$. In Fig. 5, we depict the variation of the absorption cross-section for these different values of η upon energy. The values of λ_{max} of L-mode increases from 686.88nm to 1039.88nm . The simulated absorption spectra obtained at various aspect ratios show a red shift of the λ_{max} -position, when the latter increases. These curves indicate that, for a given length, there is an aspect ratio for which the intensity of Plasmon Band is maximum. Hence, η is the key parameter of the study of the optical properties of Gold nanorods. A common observation from electron microscopy (used for the determination of the particle size) of Gold nanocrystals with spectral measurements, is an almost linear correlation between the peak-position and the aspect ratio. Results from a recent experiment (e.g. [66]) are reproduced in Fig. 6, showing that the comparison between FEM and experiment is satisfactory.

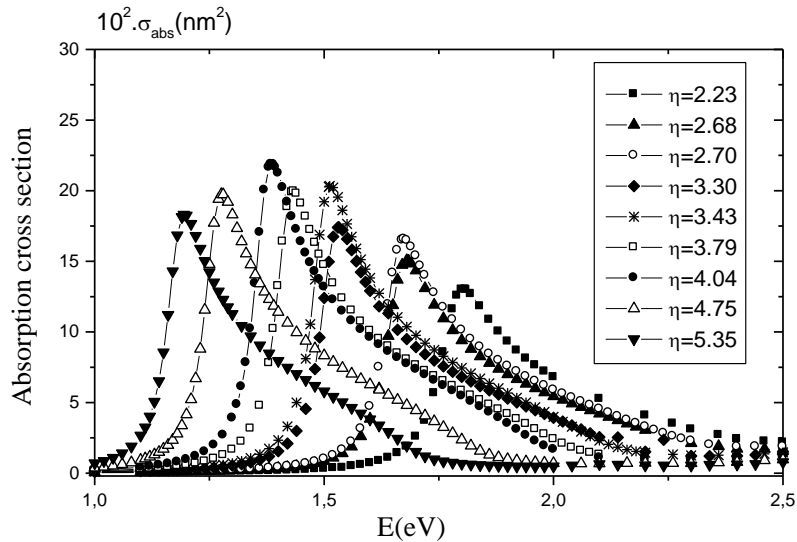


Fig. 5: Absorption spectrum of L-mode of Gold nanorods with an aspect ratio increasing from 2.23 to 5.35. The curves are drawn choosing : $\epsilon_m = 1.77$.

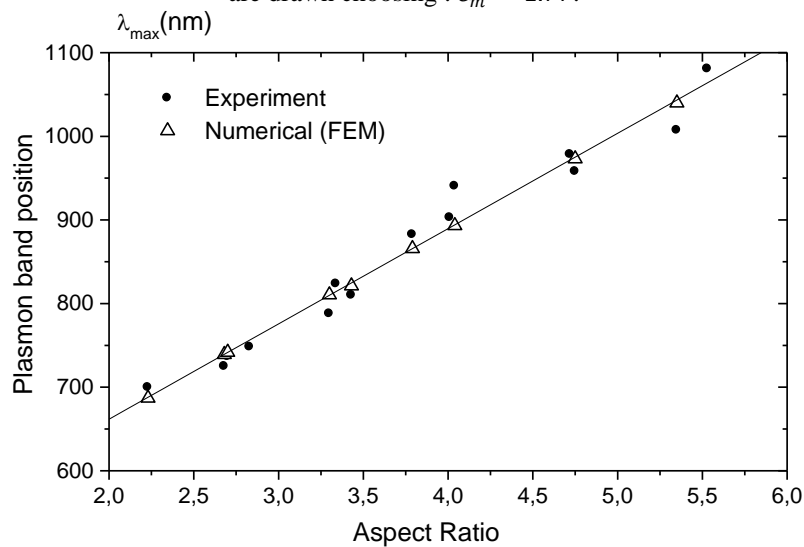


Fig. 6: A comparison between numerical and experimental plots of the surface plasmon longitudinal band position, versus the aspect ratio for pure Gold nanorods in water.

The influence of the dielectric constant of the surrounding medium is now taken into account. It is well known that the Gold nanorods change color when they are embedded in different solvents of varying refractive index, which is related to the dielectric constant by relationship (13). The simulated absorption spectra are plotted in Fig. 7, for various dielectric constants of medium. The chosen aspect ratio is $\eta = 2.28$. This figure indicates that, for Au nanorods with fixed geometrical parameters, the positions of the resonance maximum, λ_{max} , of the L-mode show a drastic red shift with increasing dielectric constants of medium, along with an increase of the absorption intensity.

For validating the simulation results, typical experimental data (e.g. [47]) are shown in Fig. 8, in which we represented the change of the Plasmon Band position, λ_{max} , of L-mode, as a function of the dielectric constant of the surrounding medium. In this figure, we report the results obtained by FEM. This clearly demonstrates that the relation between the absorption maximum of L-mode and the medium dielectric constant can be regarded as linear. This is an important

conclusion, because it cannot be seen directly considering Eq. (4). It especially shows that the effect of the medium dielectric constant should not be underestimated. We must note that the numerical results are in agreement with those of experiment.

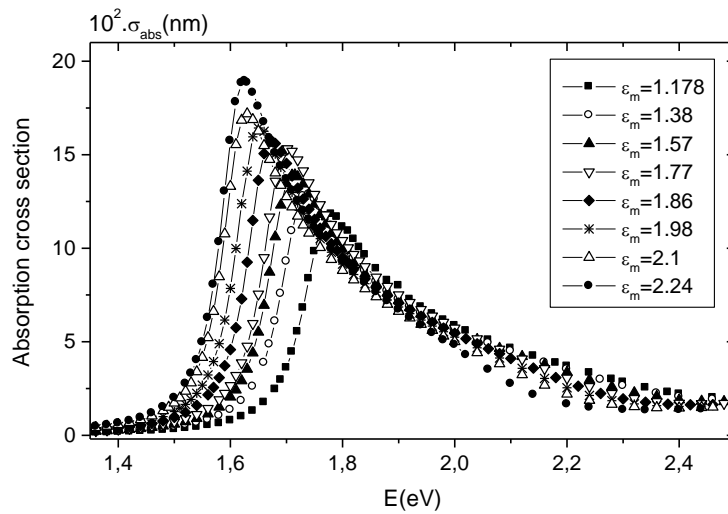


Fig. 7: Absorption spectrum of L-mode L of Gold nanorods with various values of the dielectric constant of the surrounding medium. These curves are drawn choosing : $\eta = 2.28$ and $h = 30nm$.

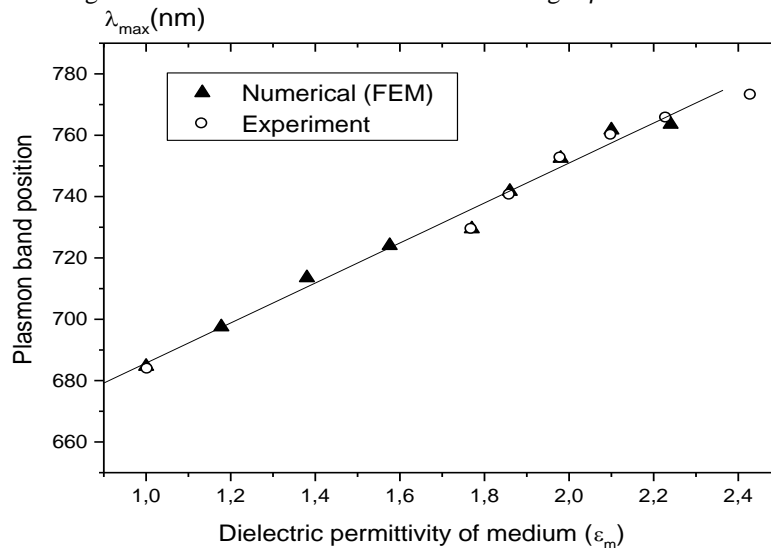


Fig. 8: A comparison between numerical and experimental plots of the surface plasmon longitudinal band position, versus the dielectric constant of the medium, for pure Gold nanorods with : $\eta = 2.28$ and $h = 30nm$.

VII. CONCLUDING REMARKS

We recall that the present work dealt with Au nanorods. Our initial motivation can be justified by the fact that these nanomaterials promise new fascinating applications including sensing, biological imaging, optical and optoelectronic devices, and clean energy. Our preferential choice of nanorods instead of nanospheres can be understood as follows. As predicted by Gans's theory (e.g. [9]), when the shape of Gold nanoparticles changes from a sphere to a rod, the SPRs band is split into two bands: a strong band in the region corresponding to electron oscillations along the long axis, referred to as longitudinal band (LB), and a weak band in the visible region at a wavelength similar to that of Gold nanospheres, referred to as transversal band (TB). The latter is insensitive to the size change, while LB is red shifted largely from the visible to near-infrared region with increasing aspect ratio. A significant change in the plasmon spectra in response to a variation of the dielectric permittivity, in the vicinity of the Gold nanorods, arises from the localized surface plasmon resonance (LSPR) properties and can be effectively utilized in Cancer imaging and Photothermal Therapy (e.g. [67]). Recently, LSPR has been applied to the detection of DNA and other biomolecules using an analyte-induced aggregation/assembly of Gold nanospheres (e.g. [68]). Although the methodology is simple and relatively straightforward, the use of Gold nanorods to detect biomolecules has obvious advantages compared to the use of Gold nanospheres. The analyte-induced aggregation of spherical Gold nanoparticles results in a decrease in the plasmon absorption at around $520nm$ and formation of a long wavelength band. It introduces significant widening in the plasmon peak thereby reducing the spectral resolution which compromises specific detection (e.g. [69]). In contrast, anisotropic Gold nanorods offer both lateral and axial (end-to-end) configurations that give rise to unique transversal and longitudinal plasmon resonance absorption. The longitudinal plasmon response to changes in the dielectric properties or

refractive indices manifests itself in characteristics resonance absorption bands in visible to IR range. This makes Gold nanorods more attractive in simple, rapid, and selective sensing in bioanalytical chemistry. The main purpose of this paper was a quantitative investigation of the absorption spectra of Au nanorods, for various shapes and forms of particles and the dielectric properties of the host medium. To this end, we have introduced a numerical modeling based on FEM, in order to compute the optical absorption and scattering of Gold anisotropic inclusions embedded in a dielectric medium. Such a method is known to be a very useful and versatile computational tool for particles with any arbitrary shape and embedded in a dielectric matrix. In particular, the study revealed that the absorption spectra are mainly governed by the longitudinal dipolar mode, that is, by the aspect ratio of the nanorods. As pointed out before, the simulation results presented in this paper were found to be in good agreement with very recent experimental data. Then, FEM approach provides a powerful tool for the study of the optical properties of nanorods.

Finally, we emphasize that the numerical method developed in this work, for the investigation of the optical properties of the rods nanogolds, can be extended to other types of Gold nanoparticles, such as noble metallic nanoalloys of different sizes and shapes, nanoshells, nanocages and nanotips, in order to improve the optical properties suitable for the biomedical applications. In addition, we emphasize that the numerical method, developed in this paper, can be extended to investigate the electromagnetic coupling between particles and its effect on the plasmonic behaviors. Such considerations are in progress.

ACKNOWLEDGMENTS

One of us (M.B.) would like to thank Professors A.R. Sennoudi and A. Boussaid for helpful discussions and the *Tlemcen University* of Algeria for their kind hospitality during its regular visits.

REFERENCES

- [1] W.H. Yang, G.C. Schatz and R.P. Van Duyne, "Discrete Dipole Approximation for Calculating Optical Absorption Spectra and Surface-Enhanced Raman Intensities for Adsorbates on Metal Nanoparticles with Arbitrary Shapes," *J. Chem. Phys.*, vol. 103, pp. 869–875, 1999.
- [2] N. Féridj, J. Aubard and G. Lévi, "Discrete Dipole Approximation for Calculating Optical Absorption Spectra and Surface-Enhanced Raman Intensities for Adsorbates on Metal Nanoparticles with Arbitrary Shapes," *J. Chem. Phys.*, vol. 111, pp. 1195–1208, 1999.
- [3] S. Link, M.A. El-Sayed and M.B. Mohamed, "Simulation of the optical absorption spectra of gold nanorods as a function of their aspect ratio and the effect of the medium dielectric constant," *J. Chem. Phys. B*, vol. 109, pp. 10531–10532, 2005.
- [4] A. Brioude, X.C. Jiang and M.P. Pileni, "optical properties of gold nanorods: DDA simulations supported by experiments," *J. Chem. Phys. B*, vol.109, pp. 13138-13142, 2005.
- [5] R.D. Averitt, D. Sarkar and N.J. Halas, "Plasmon resonance shifts of Au-coated Au₂S nanoshells: insights into multicomponent nanoparticles growth," *Phys. Rev. Letters*, vol. 78, pp. 4217–4220, 1997.
- [6] E. Prodan, C. Radloff, N. J. Halas, and P. Nordlander, "A hybridization model for the plasmon response of complex nanostructures," *Science*, vol. 302, pp. 419-422, 2003.
- [7] M. Hu *et al*, "Gold nanostructures: engineering their plasmonic properties for biomedical applications," *Chem. Soc. Rev.*, vol. 78, pp. 4217–4220, 1997.
- [8] G. Mie, "Beitrage zur Optik truber Medien, speziell kolloidaler Metallosungen," *Ann. Phys.*, vol. 25, pp. 377-445, 1908.
- [9] R. Gans, "Form of ultramicroscopic particles of silver," *Ann. Phys.*, vol. 47, pp. 270–284, 1915
- [10] M. Kerker, *The Scattering of Light and Other Electromagnetic Radiation*, Academic Press, New York, 1969.
- [11] C.F. Bohren and D.R. Huffman, *Absorption and Scattering of Light by Small Particles*, John Wiley, New York, 1983.
- [12] U. Kreibig and M. Vollmer, *Optical Properties of Metal Clusters*, Springer, Berlin, 1995.
- [13] J.C. Maxwell-Garnett, "Colours in metal glasses and in metallic films," *Phil. Trans. R. Soc. London*, vol. 203, pp.385-420, 1904.
- [14] C.A. Foss, G.L. Hornyak, M.J. Tierney and C.R. Martin, "Template synthesis of infrared-transparent metal microcylinders: comparison of optical properties with the predictions of effective medium theory," *J. Phys. Chem.*, vol. 96, pp 9001–9007, 1992.
- [15] C.A. Foss, G.L. Hornyak, J.A. Stockert and C.R. Martin, "Template-Synthesized Nanoscopic Gold Particles: Optical-Spectra and the Effects of Particle-Size and Shape," *J. Phys. Chem.*, vol. 98, pp.2963-2971, 1994.
- [16] S.A. Maier, P.G. Kik and H.A. Atwater, "Optical pulse propagation in metal nanoparticle chain waveguides," *Phys. Rev. B*, vol. 67, pp.205402(1-5), 2003.
- [17] M.S. Min, T.W. Lee, P.F. Fisher and S.K. Gray, "Fourier spectral simulation and Gegenbauer reconstructions for electromagnetic wave in the presence of a metal nanoparticle," *J. Comput. Phys.*, vol. 213, pp. 730–747, 2006.
- [18] E. Moreno, D. Erni, Ch. Hafner, and R. Vahldieck, "Multiple multipole method with automatic multipole setting applied to the simulation of surface plasmons in metallic nanostructures," *J. Opt. Soc. Am. A*, vol. 19, pp. 101-111, 2002.
- [19] J.P. Kottmann, O.J.F. Martin, D.R. Smith, and S. Schultz, "Spectral response of Silver nanoparticles," *Optics Exp.*, vol. 6, pp. 213–219, 2000.
- [20] C. Rockstuhl, M.G. Salt and H.P. Herzig, "Application of the boundary-element method to the interaction of light with single and coupled metallic nanoparticles," *J. Opt. Soc. Am. A*, vol. 20, pp. 1969-1973, 2003.

- [21] L. Rogobete and C. Henkel, "Spontaneous emission in a subwavelength environment characterized by boundary integral equations," *Phys. Rev. A*, vol. 70, pp. 063815(1-10), 2004.
- [22] F.J. Garcia de Abajo and A. Howie, "Retarded field calculation of electron energy loss in inhomogeneous dielectrics," *Phys. Rev. B*, vol. 65, pp. 115418 (1-17), 2002.
- [23] J.-W. Liaw, "Analysis of the surface plasmon resonance of a single core-shelled nanocomposite by surface integral equations," *Engineering Analysis with Boundary Elements*, vol. 30, pp. 734-745, 2006.
- [24] K.L. Kelly, E. Coronado, L.L. Zhao and G.C. Schatz, "The optical properties of metal nanoparticles : the influence of size, shape, and dielectric environment," *J. Phys. Chem. B*, vol. 107, pp. 668-677, 2003.
- [25] R. Jin et al, "Controlling anisotropic nanoparticle growth through plasmon excitation," *Nature*, vol. 425, 487-490, 2003.
- [26] S. Sadhan, S. Priyanka, P. Santanu, P.S. Gobinda and M. Ajay, "Synthesis of silver nanodiscs and triangular nanoplates in PVP matrix: Photophysical study and simulation of UV-vis extinction spectra using DDA method," *Journal of Molecular Liquids*, vol. 165, 21-26, 2012.
- [27] A. Filankembo and M.P. Pileni, "Shape control of copper nanocrystals," *Appl. Surf. Sci.*, vol. 164, pp. 260-267, 2000.
- [28] J.N. Reddy, *An Introduction to Finite Element Method*, McGraw-Hill Inc. 1993; O.C. Zienkiewicz and R.L. Taylor, *The Finite Element Method*, Vol. 1, McGraw-Hill, London, 1989.
- [29] A.R. Senoudi, F. Lallam, A. Boussaid and M. Benhamou, "numerical study of the effects of polymeric shell on plasmonic resonance of nanogolds," *International Journal of Academic Research*, vol. 2, pp. 70-78, 2010; M. Benhamou, A.R. Senoudi, F. Lallam, A. Boussaid and A. Bensafi, "Optical Properties Of Anisotropic Nanogolds From Finite Element Method," *Science & Nano Technology: An Indian Journal*, vol. 4(2), 2010.
- [30] A. Akouibaa et al, "Numerical study of the plasmonic resonance of multi-phases nanoparticles," *International Journal of Academic Research*, vol. 4, pp. 213-223, 2012.
- [31] C. Kittel, *Introduction to Solid State Physics*, Wiley, New-York, 1956.
- [32] L.M. Liz-Marzan et al., *Handbook of Surfaces and Interfaces of Materials: Core-Shell Nanoparticles and Assemblies Thereof*, vol. 3, Chap. 5, Academic Press, San Diego, 2001.
- [33] S. Link and M.A. El-Sayed, "Spectral Properties and Relaxation Dynamics of Surface Plasmon Electronic Oscillations in Gold and Silver Nanodots and Nanorods," *J. Phys. Chem. B*, vol. 103, pp. 8410-8426, 1999
- [34] U. Kreibig and L. Genzel, "Optical absorption of small metallic particles," *Surf. Sci.*, vol. 156, pp. 678-700, 1985.
- [35] P. Mulvaney, "Surface Plasmon spectroscopy of nanosized metal particles," *Langmuir*, vol. 12, pp. 788-800, 1996.
- [36] R. Ruppin, "Optical properties of a spatially dispersive cylinder," *J. Opt. Soc. Am. B*, vol.6, 1559-1563, 1989.
- [37] R. Ruppin, "Electromagnetic scattering from finite dielectric cylinders," *J. Phys. D: Appl. Phys.*, vol. 23, pp. 757-763 1990.
- [38] R. Fuchs, "Theory of the optical properties of ionic crystal cubes," *Phys. Rev. B*, vol. 11, pp. 1732-1740, 1975.
- [39] N.A.F. Al-Rawashdeh, M.L. Sandrock, C.J. Seugling and C.A. Foss, "Visible Region Polarization Spectroscopic Studies of Template-Synthesized Gold Nanoparticles Oriented in Polyethylene," *J. Phys. Chem. B*, vol. 102, pp. 361-371, 1998.
- [40] R. Ruppin, "Polariton modes of spheroidal microcrystals," *J. Phys.: Condens. Matter*, vol. 10, pp. 7869-7878 1998
- [41] B.T. Draine and P.J. Flatau, "Discrete-dipole approximation for scattering calculations," *J. Opt. Soc. Am. A*, vol. 11, pp. 1491-1499, 1994.
- [42] B.T. Draine and J. Goodman, "Beyond Clausius-Mossotti Wave propagation on a polarizable point lattice and the discrete dipole approximation," *Astrophys. J.*, vol. 405, pp. 685-697, 1993.
- [43] I.O. Sosa, C. Noguez and R.G. Barrera, "Optical properties of metal nanoparticles with arbitrary shapes," *J. Phys. Chem. B*, vol. 107, pp. 6269-6275, 2003.
- [44] I. Liseicki, F. Billoudet and M.P. Pileni, "Control of the shape and the size of copper metallic particles," *J. Phys. Chem.*, vol. 100, pp. 4160-4166, 1996.
- [45] S. Link, M.B. Mohamed and M.A. El-Sayed, "Simulation of the Optical Absorption Spectra of Gold Nanorods as a Function of Their Aspect Ratio and the Effect of the Medium Dielectric Constant," *J. Phys. Chem. B*, vol. 103, pp. 3073-3077, 1999.
- [46] S.D. Stookey and R.J. Araujo, "Selective Polarization of Light Due to Absorption by Small Elongated Silver Particles in Glass," *Appl. Opt.*, vol. 7, pp. 777-779, 1968.
- [47] J. Pérez-Juste, I. Pastoriza-Santos, L.M. Liz-Marzán and P. Mulvaney, "Gold Nanorods: Synthesis, Characterization and Applications," *Coord. Chem. Rev.*, vol. 249, pp. 1870-1901, 2005.
- [48] Y.Y. Yu, S.S. Chang, C.L. Lee, and C.R.C. Wang, "Gold nanorods: electrochemical synthesis and optical properties," *J. Phys. Chem. B*, vol. 101, pp. 6661-6664, 1997.
- [49] S.S. Chang et al, "The Shape Transition of Gold Nanorods," *Langmuir*, vol. 15, pp. 701-709, 1999.
- [50] B. Nikoobakht and M.A. El-Sayed, "Preparation and Growth Mechanism of Gold Nanorods (NRs) Using Seed-Mediated Growth Method," *Chem. Mater.*, vol. 15, pp. 1957-1962, 2003.
- [51] N.R. Jana, L. Gearheart and C.J. Murphy, "Wet Chemical Synthesis of High Aspect Ratio Cylindrical Gold Nanorods," *J. Phys. Chem. B*, vol. 105, pp. 4065-4067, 2001.
- [52] A. Silhvola and J.A. Kong, "Effective permittivity of dielectric mixtures," *IEEE T. Geosci. Remote Sensing*, vol. 26, pp. 420-429, 1988.

- [53] R. Kubo, A. Kawabata and S. Kobayashi, "Electronic Properties of Small Particles," *Ann. Rev. Mater. Sci.*, vol. 14, pp. 49-66, 1984.
- [54] V.P. Drachev et al, "The Ag dielectric function in plasmonic metamaterials," *Optics Express*, vol. 16, pp. 1186-1195, 2008.
- [55] M.M. Alvarez *et al*, "Optical Absorption Spectra of Nanocrystal Gold Molecules. *J. Phys. Chem. B*, vol. 101, 3706-3712, 1997.
- [56] G. Weick, R.A. Molina, D. Weinmann and R.A. Jalabert, "Lifetime of the first and second collective excitations in metallic nanoparticles," *Phys. Rev. B*, vol. 72, pp. 115410(1-17), 2005.
- [57] A Vial and T. Laroche, "Description of dispersion properties of metals by mean of the critical points model and application to the study of resonant structures using the FDTD method," *J. Phys. D: Appl. Phys.*, vol. 40, pp. 7152-7158, 2007.
- [58] A. Vial and T. Laroche, "Comparison of gold and silver dispersion laws suitable for FDTD simulations," *Appl. Phys. B-Lasers Opt.*, vol. 93, pp. 139-143, 2008.
- [59] E.D. Palik (ed.), *Handbook of Optical Constants of Solids III*, Academic Press, New York, 1991.
- [60] L. Jylhä and A. Sihvola, "Numerical modeling of disordered mixture using pseudorandom simulations," *IEEE Tran. Geosci. and Remote Sensing*, vol. 43, pp. 59-64, 2005.
- [61] K. Kärkkäinen, A. Sihvola and K. Nikoskinen, "Analysis of a three-dimensional dielectric mixture with finite difference method," *IEEE Trans. Geosci. Remote Sensing*, vol. 39, pp. 1013-1018, 2001.
- [62] V. Myroshnychenko and C. Brosseau, "Finite-element modeling method for the prediction of the complex effective permittivity of two-phase random statistically isotropic heterostructures," *J. Appl. Phys.*, vol. 97, pp. 044101(1-14), 2005.
- [63] V. Myroshnychenko and C. Brosseau, "Finite-element method for calculation of the effective permittivity of random inhomogeneous media," *Phys. Rev. E*, vol. 71, pp. 016701(1-16), 2005.
- [64] A. Mejdoubi and C. Brosseau, "Finite-element simulation of the depolarization factor of arbitrarily shaped inclusions," *Phys. Rev. E*, vol. 74, pp. 031405(1-13) 2006.
- [65] X.C. Jiang, A. Brioude and M.P. Pileni, "Gold Nanorods: Limitations in their Syntheses and Optical Properties," *Colloids and Surfaces A*, vol. 277, pp. 201-206, 2006.
- [66] J. Pérez-Juste *et al*, "Electric-Field-Directed Growth of Gold Nanorods in Aqueous Surfactant Solutions," *Adv. Funct. Mater*, vol. 14, pp. 571-579, 2004.
- [67] X. Huang and M.A. El-Sayed, "Gold nanoparticles: Optical properties and implementations in cancer diagnosis and photothermal therapy," *Journal of Advanced Research*, vol. 1, pp. 13-28, 2010.
- [68] Z. Ma, L. Tian, T. Wang and C. Wang, "Optical DNA detection based on gold nanorods aggregation," *Anal. Chim. Acta*, vol. 673, pp. 179-84, 2010.
- [69] J.S. Lee, P.A. Ulmann, M.S. Han and C.A. Mirkin, "A DNA-Gold Nanoparticle Based Colorimetric Competition Assay for the Detection of Cysteine," *Nano Lett.*, vol. 8, pp. 529-533, 2008.